ASPECTS OF THREE-DIMENSIONAL MAGNETIC RECONNECTION

(Invited Review)

E. R. PRIEST[1] and C. J. SCHRIJVER[2]
[1]*Department of Mathematical Sciences, St. Andrews University, St. Andrews KY16 9SS, Scotland (eric@mcs.st-and.ac.uk)*
[2]*Lockheed Palo Alto Research Laboratory, 3251 Hanover Street, Palo Alto, CA 94304-1191, U.S.A. (schrijver@lmsal.com)*

(Accepted 5 November 1999)

Abstract. In this review paper we discuss several aspects of magnetic reconnection theory, focusing on the field-line motions that are associated with reconnection. A new exact solution of the nonlinear MHD equations for *reconnective annihilation* is presented which represents a two-fold generalization of the previous solutions. Magnetic reconnection at null points by several mechanisms is summarized, including *spine reconnection*, *fan reconnection* and *separator reconnection*, where it is pointed out that two common features of separator reconnection are the rapid flipping of magnetic field lines and the collapse of the separator to a current sheet. In addition, a formula for the rate of reconnection between two flux tubes is derived. The magnetic field of the corona is highly complex, since the magnetic carpet consists of a multitude of sources in the photosphere. Progress in understanding this complexity may, however, be made by constructing the *skeleton* of the field and developing a theory for the local and global bifurcations between the different topologies. The eruption of flux from the Sun may even sometimes be due to a change of topology caused by *emerging flux break-out*. A CD-ROM attached to this paper presents the results of a toy model of vacuum reconnection, which suggests that rapid flipping of field lines in fan and separator reconnection is an essential ingredient also in real non-vacuum conditions. In addition, it gives an example of *binary reconnection* between a pair of unbalanced sources as they move around, which may contribute significantly to coronal heating. Finally, we present examples in TRACE movies of geometrical changes of the coronal magnetic field that are a likely result of large-scale magnetic reconnection.

1. Introduction

Magnetic reconnection is a common phenomenon in the solar corona. Its presence is most easily inferred indirectly from the formation of connections between bipolar regions that emerged at different locations and times. These connections range in lengths from hundreds of thousands of kilometers for coronal loops between distant active regions – many even crossing the equator – down to only thousands of kilometers in so-called coronal bright points that form between magnetic concentrations in the quiet-Sun network. For example, we refer to TRACE movies by Schrijver *et al.* (1999) for a detailed movie of an emerging active region, and to EIT/MDI studies of coronal bright points by Schrijver *et al.* (1997). These studies show that regions as far apart as $\approx 10^5$ km can reconnect within about 10–12 hours, even if the fields in question are not forced together very closely in the

Solar Physics **190:** 1–24, 1999.

solar surface. These and past studies with, for example, *Skylab* and *Yohkoh*, have demonstrated that apparently the mere presence of distant fields inevitably leads to reconnection.

The high-resolution, high-cadence TRACE observations (see Handy *et al.*, 1999 for a description of the instrument) add new information because we can actually see loops deform and bend towards the nearby field. Even the macroscopic consequences of actual reconnection in progress still escapes detection, because generally loops fade in a matter of hours or even less, only to reappear in one of the narrow thermal pass-bands visible to TRACE. This is generally after the reconnection has been completed and the new loops are in place, roughly in the shape they will retain for some time after the reconnection.

Both the observational and theoretical aspects of reconnection are huge subjects, as can be seen from the vast literature on them (see a new book by Priest and Forbes, 2000, for references). In this review we shall be able to touch on a few aspects only briefly. Section 2 presents some new exact solutions, while Section 3 describes the mechanisms for reconnection at a three-dimensional null point where the magnetic field vanishes. Then Section 4 discusses the highly complex topology of the coronal magnetic field and Section 5 presents a simple toy model for vacuum reconnection in response to the motion of magnetic sources in the solar surface.

2. Exact Solutions for Steady Two-Dimensional Flow

While most of this paper is concerned with three-dimensional reconnection, the search for exact solutions is one of the key remaining areas of two-dimensional reconnection that remains to be developed.

We have been having fun for the past couple of months looking with Slava Titov for new exact solutions of the steady two-dimensional MHD equations, namely Ohm's law

$$\mathbf{E} + \mathbf{v} \times \mathbf{B} = \eta \nabla \times \mathbf{B} \,, \tag{1}$$

where $\mathbf{E}$ is the (uniform) electric field, $\mathbf{v}$ the plasma velocity, $\mathbf{B}$ the magnetic field and η the magnetic diffusivity, and the equation of motion

$$\rho(\mathbf{v} \cdot \nabla)\mathbf{v} = -\nabla\left(p + \frac{B^2}{2\mu}\right) + (\mathbf{B} \cdot \nabla)\frac{\mathbf{B}}{\mu} \,, \tag{2}$$

where p is the plasma pressure, ρ the density (assumed constant), and

$$\nabla \cdot \mathbf{B} = \nabla \cdot \mathbf{v} = 0 \,.$$

2.1. Magnetic annihilation

The simplest exact solution is for magnetic annihilation and has been known for a long time (Sonnerup and Priest, 1975). A stagnation-point flow

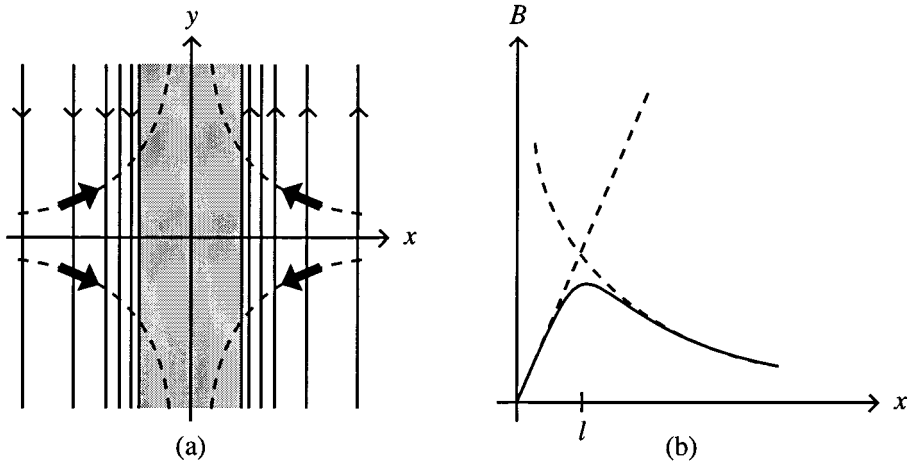

Figure 1. (a) The magnetic field lines (solid) and streamlines (dashed) for magnetic annihilation. The region of strong current is shaded and has a width $2l$. (b) The resulting magnetic field profile.

$$v_x = v_{xe}x, \qquad v_y = -v_{xe}y \tag{3}$$

(with v_{xe} constant) carries in a unidirectional magnetic field

$$\mathbf{B} = B(x)\hat{\mathbf{y}} \tag{4}$$

towards the origin (Figure 1), where a one-dimensional current $j(x)$ is concentrated. Equation (2) is satisfied identically and Ohm's law (1) becomes

$$E + v_{xe}xB = \eta\frac{\mathrm{d}B}{\mathrm{d}x}\ ,$$

which determines the unknown function $B(x)$ as

$$B(x) = B_{ye}\sqrt{\frac{-2v_{xe}}{\eta}}\ \mathrm{daw}\left(x\sqrt{\frac{-v_{xe}}{2\eta}}\right) \tag{5}$$

in terms of the Dawson integral function

$$\mathrm{daw}(X) = e^{-X^2}\int_0^X e^{t^2}\,\mathrm{d}t\ .$$

For this solution, it is possible to prescribe the x-component of velocity (v_{xe}) and y-component of magnetic field (B_{ye}) at a fixed point ($x = 1$, say) on the y-axis.

2.2. Reconnective annihilation

Much more recently, Craig and Henton (1995) generalized this to give a solution for reconnective annihilation by adding new terms to (3) and (4) to give

$$v_x = v_{xe}x, \quad v_y = -v_{xe}y - \frac{v_{ye}}{B_{ye}}A_0'(x) \ , \tag{6}$$

and

$$B_x = v_{xe}\frac{v_{ye}}{B_{ye}}x, \quad B_y = -v_{xe}\frac{v_{ye}}{B_{ye}}y - A_0'(x) \ . \tag{7}$$

The equation of motion is again satisfied identically by this form and Ohm's law determines the unknown function $A_0'(x)$ to be

$$A_0'(x) = -\frac{E}{\eta\lambda}\ \mathrm{daw}\ (\lambda x) \ , \tag{8}$$

where

$$\lambda^2 = \frac{E}{2\eta B_{ye}} \ .$$

The current $j(x)$ is still in the form of a one-dimensional sheet and the streamlines represent an asymmetric stagnation-point flow that carries the field lines into the sheet and reconnects them there (Figure 2).

In this case the y-component of velocity (v_{ye}) may be prescribed at $(1, 0)$ in addition to v_{xe} and B_{ye}. In terms of a stream function (ψ) and flux function (A), such that

$$(v_x, v_y) = \left(\frac{\partial\psi}{\partial y}, -\frac{\partial\psi}{\partial x}\right), \quad (B_x, B_y) = \left(\frac{\partial A}{\partial y}, -\frac{\partial A}{\partial x}\right) \ ,$$

the solutions are

$$A = A_0(x) + v_{xe}\frac{v_{ye}}{B_{ye}}xy \ , \tag{9}$$

$$\psi = \frac{v_{ye}}{B_{ye}}A_0(x) + v_{xe}xy \ , \tag{10}$$

which represent linear combinations of the one-dimensional $(A_0(x))$ and hyperbolic (xy) forms.

2.3. More general exact solutions

We were fortunate to discover much more general exact solutions of the form

$$A = A_0(x) + A_1(x)y \ , \tag{11}$$

$$\psi = \psi_0(x) + \psi_1(x)y \ , \tag{12}$$

involving four unknown functions of x. It transpires that Ohm's law reduces to two equations for these functions and the equation of motion implies another two functions. Furthermore, we can prescribe B_x as B_{xe} at $(1, 0)$ in addition to imposing v_{xe}, v_{ye}, B_{ye} and we can also prescribe the value of a parameter γ. The Craig–Henton solution has $B_{xe} = v_{xe}v_{ye}/B_{ye}$ and $\gamma = 1$.

With the form (11) and (12) Ohm's law becomes

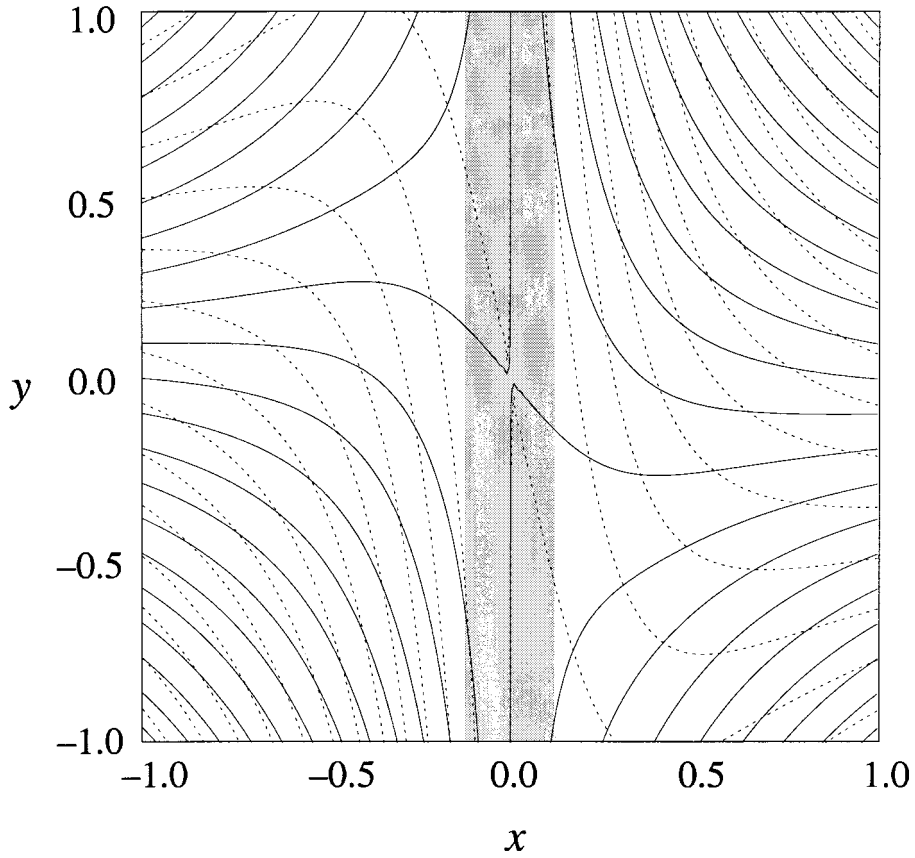

Figure 2. The field lines (dashed) and streamlines (solid) for reconnective annihilation. An asymmetric stagnation point flow brings field lines in from the two sides to an infinitely long current sheet (shaded), where they are reconnected.

$$E + \psi_1(-A_0' - A_1' y) + (\psi_0' + \psi_1' y) = \eta(-A_0'' - A_1'' y) \ ,$$

in which some terms are just functions of x and so sum to zero, while other terms are of the form y times a function of x and so they also sum to zero to give the second of the required equations. If we set the constants ρ and μ to unity for simplicity, the combination $\mathbf{M} \equiv (\mathbf{v} \cdot \nabla)\mathbf{v} - (\mathbf{B} \cdot \nabla)\mathbf{B}$ in the equation of motion has its x-component a function of x alone, while the y-component is of the form

$$M_y = f(x) + y g(x) \ .$$

Thus, the equation of motion implies partly that

$$\nabla \cdot \mathbf{M} = -\nabla^2 p \ ,$$

which determines the plasma pressure, and partly that

$$\nabla \times \mathbf{M} = \mathbf{0} \ ,$$

which implies that the above functions $f(x)$ and $g(x)$ are constants ($-l$ and $-k$, say).

The resulting four equations are

$$-\psi_1 A_1' + \psi_1' A_1 + \overline{\eta} A_1'' = 0 \,, \tag{13}$$

$$-\psi_1'^2 + \psi_1 \psi_1'' + A_1'^2 - A_1 A_1'' = k \,, \tag{14}$$

$$E - \psi_1 A_0' + \psi_0' A_1 + \eta A_0'' = 0 \,, \tag{15}$$

$$\psi_0'' \psi_1 - \psi_0' \psi_1' - A_0'' A_1 + A_0' A_1' = l \,. \tag{16}$$

The first two equations determine $\psi_1(x)$ and $A_1(x)$. They are nonlinear, but $\overline{\eta}$ is the dimensionless magnetic diffusivity (the inverse of the magnetic Reynolds number) and is very much smaller than unity. A boundary-layer solution may therefore be found by the method of matched asymptotic expansions. Equations (15) and (16) are linear in ψ_0' and A_0' and so may be solved by standard techniques. At present we are determining the properties of the solutions and extending them to three dimensions (see Priest *et al.*, 1999, for further details).

3. Reconnection at Three-Dimensional Null Points

Reconnection in two dimensions is now fairly well understood, but when we go from two dimensions to three dimensions there are many new features. For example, the structure of null points where the magnetic field vanishes is quite different (Figure 3). An isolated field line called a *spine* approaches (or leaves) the null point from above and below along the z-axis in Figure 3. Also, a set of field lines called a *fan* surface leaves (or approaches) the null from the side in the xy-plane.

Several different types of reconnection are possible in three dimensions at a null (Priest and Titov, 1996). *Spine reconnection* has the current and therefore the dissipation concentrated along the spine, whereas *fan reconnection* has them concentrated in the fan surface. When two nulls are present, their fans in the generic case intersect in a special magnetic field line called a *separator* that links from one null to another. *Separator reconnection* then tends to have the current concentrated in the separator.

These results are based largely on geometric arguments and on kinematic studies, in which the motions of field lines in response to boundary motions are analyzed. The feedback in the equation of motion of the magnetic forces associated with the presence of currents is neglected in this analysis, but it is not expected to change the present qualitative understanding from the induction equation alone.

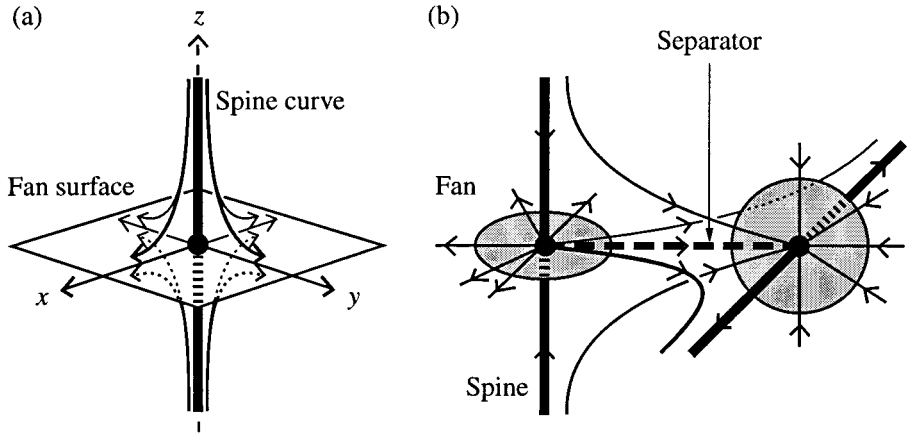

Figure 3. The structure of (a) a three-dimensional null point and (b) the separator joining two nulls. The fan surfaces are indicated schematically by shaded disks.

3.1. SPINE AND FAN RECONNECTION

Surround a null point by a cylindrical surface with its axis parallel to the spine and consider first what happens in a vertical plane through the null where the magnetic field lines have a simple X-type topology. If the footpoints of the field lines on one side move down continuously, while those on the other side move up, then the field lines in that plane will just reconnect in the classical two-dimensional manner (Figure 4(a)). A similar process takes place in all the other planes through the spine, but what happens to the flux surfaces? You form a flux surface by taking a series of footpoints on a curve and constructing the field lines through the footpoints. Suppose, for example, that you take a circle of footpoints on the curved surface of the cylinder (Figure 4(b)) and move it down continuously through the fan (Figure 4(b–d)), while another circle on the opposite side of the fan moves upward. Then two flux tubes approach one another and reconnect in the way shown in Figure 4.

In spine reconnection, you impose continuous footpoint motions across the fan and this generates a singularity along the spine. By comparison, for fan reconnection continuous footpoint motions are imposed on the top and bottom of the cylinder across the spine. This generates a singularity in the fan. The reason is that small motions of the footpoints across the top produce rapid flipping of the field line footpoints on the curved surface just above the fan around the z-axis, whereas simultaneous motions of footpoints on the top produce rapid flipping of their footpoints in the opposite direction just below the fan (Figure 5). Such flipping is associated intimately with the reconnection and is a common feature of the simple vacuum experiments described in Section 5.

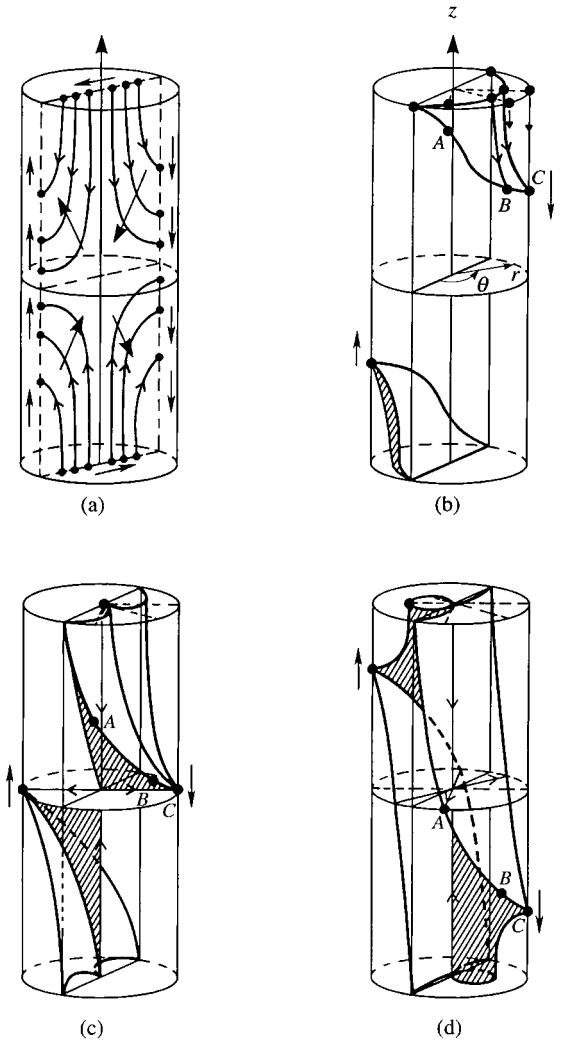

Figure 4. Spine reconnection, showing (a) motions of field lines in a plane through the spine and (b)–(d) motions of flux surfaces in response to the motions of field-line foot-points on the curved surface of a cylinder surrounding a null point with its spine (z-axis) and fan ($z = 0$ plane). As the foot-points (e.g., A, B and C) on the right-hand part of the surface move down and the corresponding points on the left-hand part move up, so two flux surfaces approach the null point (b), touch at the null point (c) and are reconnected to form two new flux tubes (d).

3.2. SEPARATOR RECONNECTION

Consider two null points with their fans intersecting in a separator (Figure 6). Just as X-points in two dimensions can collapse to form a current sheet, so in three dimensions a separator tends to collapse to a current sheet in response to footpoint motions and therefore reconnection tends to take place in it. In a plane normal to the

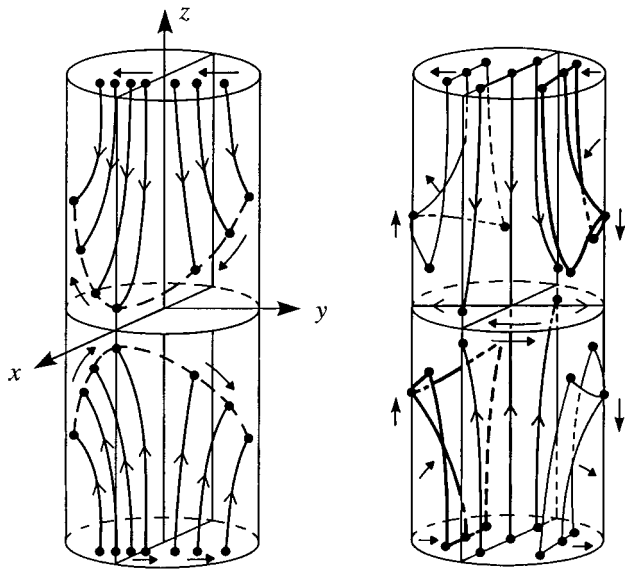

Figure 5. Fan reconnection, showing motion of (a) a field line and (b) a flux surface in response to motions of footpoints across the top and bottom boundaries of a cylinder surrounding a null point at the origin. In (a) a footpoint moves across the top of the cylinder from right to left and makes a field line (which always lies in a vertical plane through the z-axis) rotate around the z-axis. In (b) a row of footpoints parallel to the x-axis marches across the top from right to left in the negative y-direction, and the flux surface through those footpoints is distorted as it is reconnected.

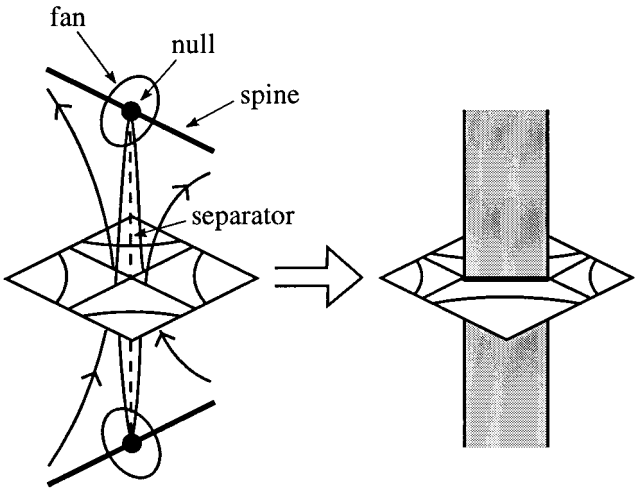

Figure 6. Collapse of a separator to form a current sheet (shaded).

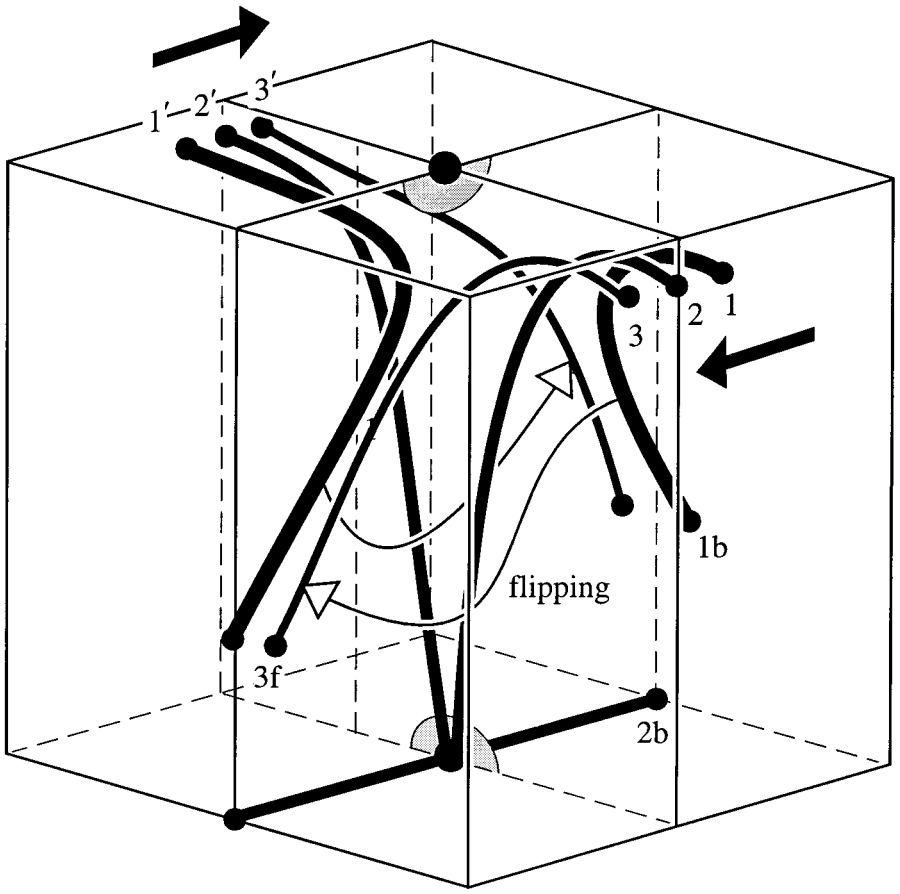

Figure 7. Rapid counter-flipping of field lines caused by small footpoint motions on the left- and right-hand sides of a box. One null point and its spine lies on the top side and another lies on the bottom of the box. Footpoints move from 1 to 2 to 3 on the right-hand side and from $1'$ to $2'$ to $3'$ on the left-hand side. This forces the field lines through those footpoints to flip from the back of the box (1b and 2b) to the front (3f), and vice-versa, and to reconnect at the lower null point.

separator, the field lines have an X-type topology (Figure 6(a)), and so when these field lines collapse they form a current sheet all along the separator (Figure 6(b)). This process may well be driven or reinforced by the natural tendency for the null points at the ends of the separator to collapse themselves (Parnell *et al.*, 1996). Also, it can be seen that the current sheet tends to be inclined at $\pi/4$ to the two fan surfaces. See Galsgaard *et al.* (paper presented at SOHO-9 Workshop in Monterey) for a numerical experiment illustrating this behavior. Once a current sheet forms, reconnection will inevitably take place, but if the sheet is small the behavior of the field lines outside the vicinity of the separator may be well described by a kinematic or vacuum model.

Suppose we surround the pair of nulls by a surface such as a cube and impose footpoint motions on the surface. Then the nature of the reconnection depends on the nature of the footpoint motions. For example, if smooth footpoint motions are imposed across both spines, then the current will tend to be concentrated in both fans and therefore especially in the separator. On the other hand, if continuous motions are imposed across the upper spine, say, and the lower fan, then fan reconnection at the upper null and spine reconnection at the lower null will occur, as in Figure 7. Here the solid field line has a footpoint that moves from point 1 to 2 to 3 on the right-hand side of the cube, while the other end rapidly flips from the back face to the front face by reconnecting at the lower null. At the same time the dashed field line has one footpoint that moves from $1'$ to $2'$ to $3'$, while its other footpoint rapidly flips in the other direction from the front face to the back face. This counter-flipping is an important feature of fan and separator reconnection.

3.3. Rate of reconnection in three dimensions

The theories for the various mechanisms for reconnection in three dimensions have not yet been developed enough to determine the rate of reconnection, but at least we can generalize the Sweet–Parker estimate from two dimensions into three dimensions. In two dimensions, one simply considers a diffusion region of width $2l$ and length $2L$ with magnetic flux being brought in from the sides with field strength B_i at a speed v_i and expelled at the Alfvén speed (v_{A}). For a steady balance between inwards advection and outwards diffusion

$$v_i = \frac{\eta}{l} , \tag{17}$$

and for a balance of mass flowing into and out of the sheet

$$v_i L = v_{\mathrm{A}} l . \tag{18}$$

Eliminating l gives the standard Sweet–Parker reconnection rate

$$v_i = \frac{v_{\mathrm{A}}}{R_m^{1/2}} , \tag{19}$$

where

$$R_m = \frac{L v_{\mathrm{A}}}{\eta}$$

is the magnetic Reynolds number based on the length of the current sheet and the Alfvén speed.

Suppose that two flux tubes of field strength B_i inclined at an angle θ are approaching one another at a speed v_i and interact in a disc-shaped current sheet of radius L and thickness $2l$. (The analysis may easily be repeated for other-shaped sheets.) As in two dimensions the speed of approach of the field lines is simply the speed of diffusion in the sheet of width l, so that

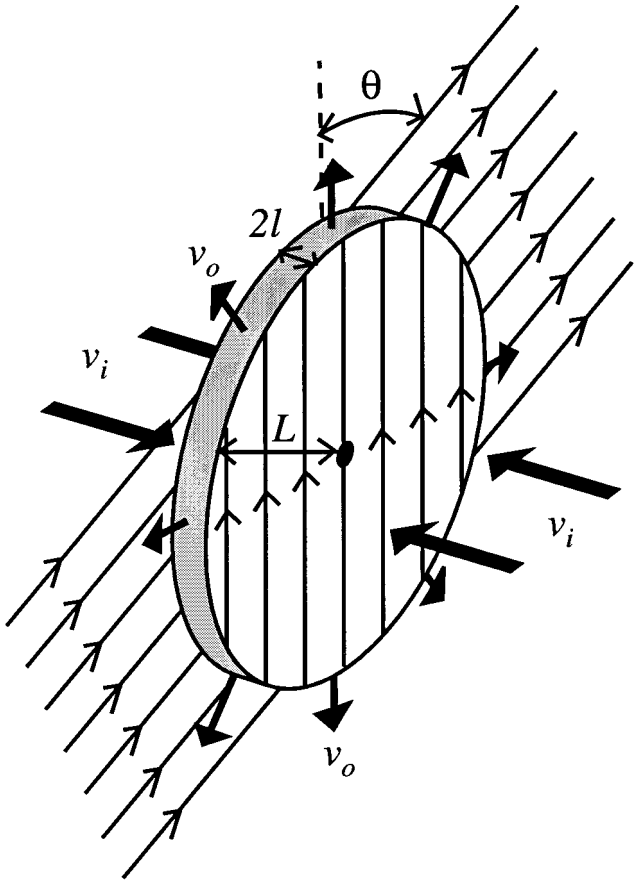

Figure 8. The three-dimensional reconnection of two flux tubes inclined at an angle θ. The field lines of one tube are shown on the front side of a disc-shaped diffusion region and of the other tube behind the disc.

$$v_i = \frac{\eta}{l} \, . \tag{20}$$

The mass entering the sheet through two surfaces of area πL^2 at speed v_i must balance the mass leaving at speed v_0, say, through the curved surface of area $2\pi L \times 2l$, and so

$$v_i \pi L^2 = 2\pi L l v_0 \, . \tag{21}$$

However, what is the outflow speed v_0? The magnetic field in the center of the sheet is $B_i \cos \frac{1}{2}\theta$ and so transverse pressure balance across the sheet as the magnetic field decreases from B_i to $B_i \cos \frac{1}{2}\theta$ implies that the pressure in the center of the sheet is enhanced by an amount

$$\frac{B_i^2}{2\mu} - \frac{B_i^2}{2\mu} \cos^2 \tfrac{1}{2}\theta = \frac{B_i^2}{2\mu} \sin^2 \tfrac{1}{2}\theta$$

over the external pressure. Such a pressure will accelerate the plasma to a speed v_0 such that

$$\tfrac{1}{2}\rho v_0^2 = \frac{B_i^2}{2\mu}\ \sin^2\tfrac{1}{2}\theta$$

as it flows from inside to outside the sheet. Thus

$$v_0 = v_{\rm A}\ \sin\tfrac{1}{2}\theta\ , \tag{22}$$

where $v_{\rm A} = B_i/\sqrt{(\mu\rho)}$.

Equations (20)–(22) therefore determine the reconnection rate as

$$v_i = \frac{v_{\rm A}}{R_m^{1/2}}\sqrt{(2\ \sin\tfrac{1}{2}\theta)}\ . \tag{23}$$

Thus, the reconnection rate varies with θ and has a maximum value (when the fields are anti-parallel) that is $\sqrt{2}$ times higher than in two dimensions, since plasma can escape from the sheet in the third dimension.

How does the shape of the current sheet affect the reconnection rate? If the circular shape is replaced by a square of side L and the flow is still axisymmetric, Equation (21) for mass conservation is replaced by

$$v_i L^2 = 2Llv_0$$

and so there is no change in the reconnection rate. On the other hand, consider a separator current sheet of width $2l$ and breadth $2L$ stretching a distance L_s along the separator from one null to another. For this, mass conservation becomes

$$v_i L_s L = v_0 l L_s$$

if the flow is roughly two-dimensional and exits the sheet in a direction perpendicular to the separator. Therefore, we recover the usual two-dimensional reconnection rate

$$v_i = \frac{v_{\rm A}}{R_m^{1/2}}\ . \tag{24}$$

This gives the reconnection rate in a sheet of given length (L), but in many applications it is the rate at which the fields approach that is given, in which case this equation simply determines the size of the current sheet as

$$L = \frac{\eta v_{\rm A}}{v_i^2} \tag{25}$$

or in dimensionless form

$$\frac{L}{L_e} = \frac{1}{M_i^2 R_{me}}\ , \tag{26}$$

where $R_{me} = L_e v_{\rm A}/\eta$ and $M_i = v_i/v_{\rm A}$ in terms of a given external scale L_e.

4. The Magnetic Topology of Coronal Magnetic Fields

On the Sun's surface there are many magnetic fragments that act as sources for the overlying coronal magnetic field and so the topology of the coronal field is extremely complex. The way to try and understand this complexity is to focus on the *skeleton* of the magnetic field, which we define to be a set of null points together with a network of spine curves and a collection of separatrix fan surfaces.

4.1. Topology due to 2, 3 or 4 sources

In two dimensions separatrix curves divide the plane up into topologically distinct regions (e.g., Figure 9(a)) in the sense that all the field lines in one region start at the same source and end at the same sink. Separatrix curves intersect in X-type null points, which are weak points in the field where current sheets tend to form and so magnetic energy is dissipated by reconnection with magnetic field lines crossing the separatrices from one region to another.

In three dimensions, in a similar way, separatrix surfaces divide the volume into regions of different topology. This time the separatrices intersect in a curve known as a *separator*, which starts at one null point and ends in another null point (Figure 9(c)). Again the null points and the separator are locations in the configuration where the magnetic energy tends to dissipate due to the creation of current sheets. Reconnection now transfers magnetic flux across the separatrix surfaces from one region to another.

We have been building up an understanding of complex topologies by considering the structure of the magnetic fields due to two, three, and four sources. For two unbalanced sources there is a null, a spine and a separatrix fan surface which arches over to form a dome from the null point to the larger source (Figure 10). This may at first sight seem to be an uninteresting case, since as the sources move about the magnetic flux joining them remains constant. However, reconnection still takes place, since individual field lines will change their connectivity, by a process referred to as *binary reconnection*. This binary interaction of pairs of unbalanced sources may well produce a substantial amount of heating in the overlying corona.

For three unbalanced sources the magnetic field is surprisingly rich, since there are six different topological states (Figure 11), the simplest of which has two separate separatrix surfaces. Transfer from one state to another is either by a *local bifurcation*, in which a pair of null points is created or destroyed or by a *global bifurcation*, when often a separator is created or destroyed without the number of null points changing (see Brown and Priest, 1999, for details).

4.2. Eruptions by emerging flux breakout

It is even possible that eruptions (to produce jets, flares or CME's) may be caused not by an instability but by a change in topology by *emerging flux breakout* (Bungey, 1995). For example, consider the two-dimensional field due to a small dipole (with

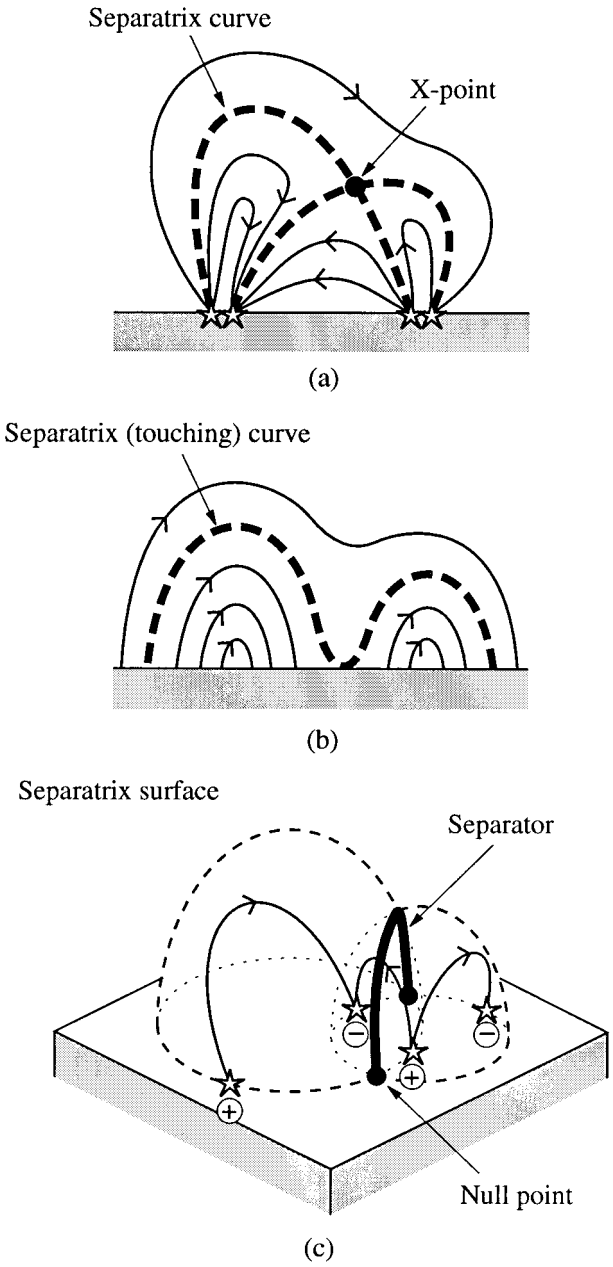

Figure 9. Separatrices in two- and three-dimensional magnetic fields.

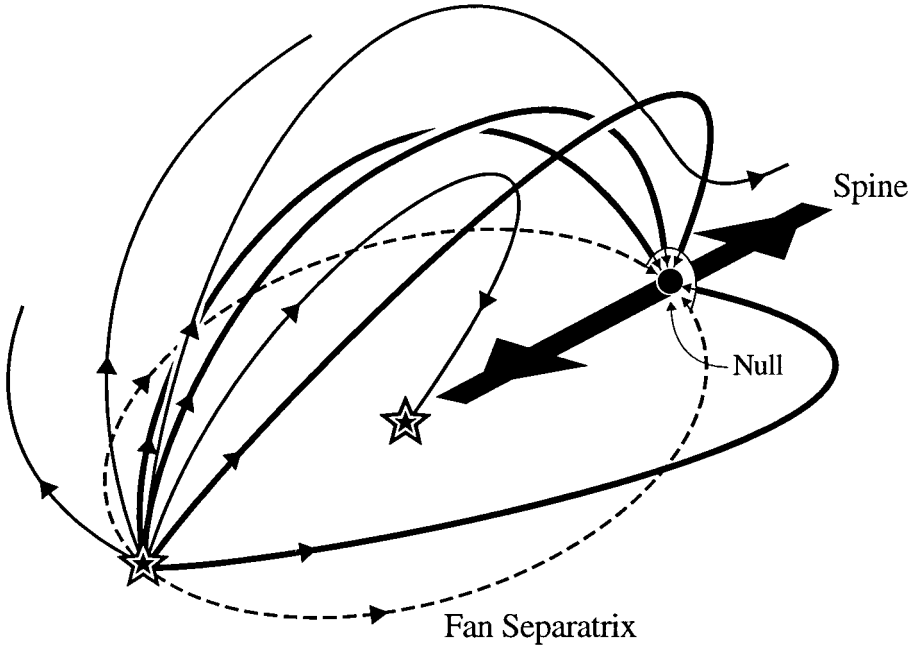

Figure 10. Skeleton of two unbalanced sources (*starred*), showing the null, the spine and field lines (*thick*) in the fan and field lines (*thin*) above and below it. The separatrix fan surface intersects the plane of the sources in the dashed curve.

sources at $\pm r_2$ on the x-axis) inside a larger dipole (with sources at ± 1 on the x-axis), as shown in Figure 12. Initially, there are two null points on the x-axis (Figure 12(a)). Now, consider what happens as the strength of the inner dipole increases due to the emergence of new flux. First of all, the nulls coalesce (Figure 12(b)) and bifurcate to a new topology with a null ring so that in a vertical plane there is an X-point above the x-axis (Figure 12(c)). As the flux continues to emerge, the field lines reconnect and the X-point rises. Eventually, it reaches infinity and there is a bifurcation to another topology shown in Figure 12(d). A similar process takes place when the sources are non-collinear, but now the X-line becomes a separator, as shown in Figure 13 where the sources on the plane are indicated by stars and the spines coming from the nulls by thick curves. Initially, the skeleton has two separate domes (Figure 13(a)) with two null points. At a critical point the nulls become connected and a separator is born by a global separator bifurcation (Figure 13(b)). Subsequently, as the flux continues to emerge, the separator, representing the intersection of the two domes, rises (Figure 13(c)) and eventually there is another global bifurcation to a new topology with the separator having erupted to infinity.

Although this model does cause flux to move outwards to infinity, it does so in a continuous manner and so does not produce the rapid reconnection and explosive rise needed for a solar eruption. Perhaps that additional feature would be present

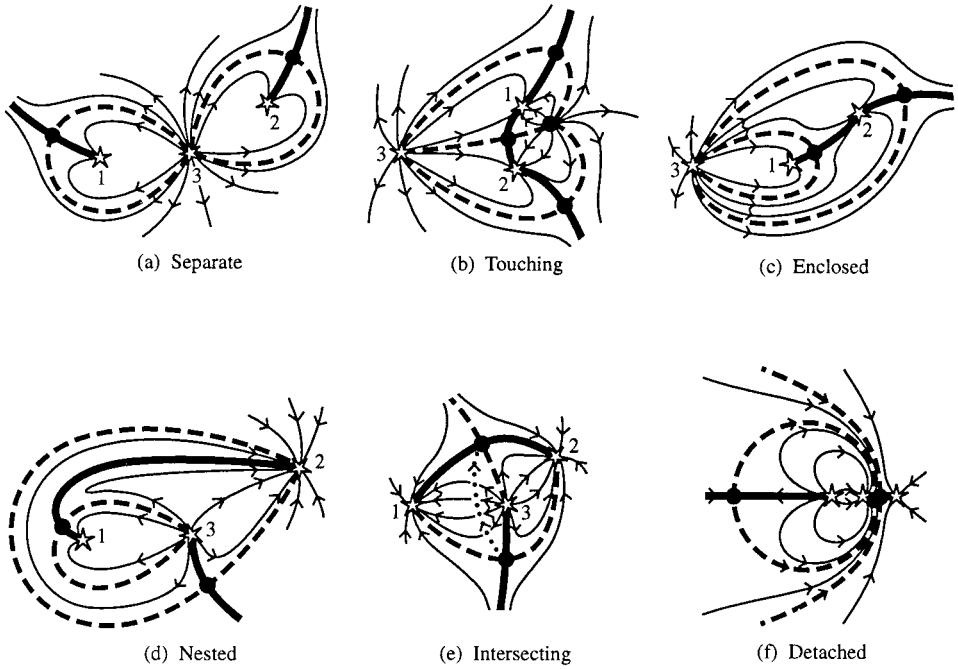

Figure 11. The magnetic topologies due to three sources seen from above. The sources are shown by stars, the nulls by large dots, the spines by thick curves and the separatrix fans by dashed curves.

in a similar force-free model, when the energy stored in closed regions could be released as they erupt.

5. Toy Model for Vacuum Reconnection

We have constructed a simple toy model for vacuum reconnection driven by the motion of photospheric sources and have presented the results in the accompanying CD-ROM. We calculate the potential magnetic field due to two, three or four sources in the solar surface and then extend it to a many-source case in which the surrounding fields generally limit the motions of the field lines in response to the footpoint motions to much smaller amplitudes than in the few-source case. The sources are slowly moved around and we assume that the field remains potential. Although this is an oversimplified model, the resulting motion of the field lines is instructive and it is a useful preliminary for a resistive MHD numerical model that we are planning to undertake.

First of all, we consider a simple model of *binary reconnection* due to the motion of two sources (Figure 14(a)). The right-hand source is the larger and it performs an orbit around the other source, during which we keep the directions constant of most of the field lines from the larger source. The way in which the field lines reconnect by changing from being open to closed and back to open can

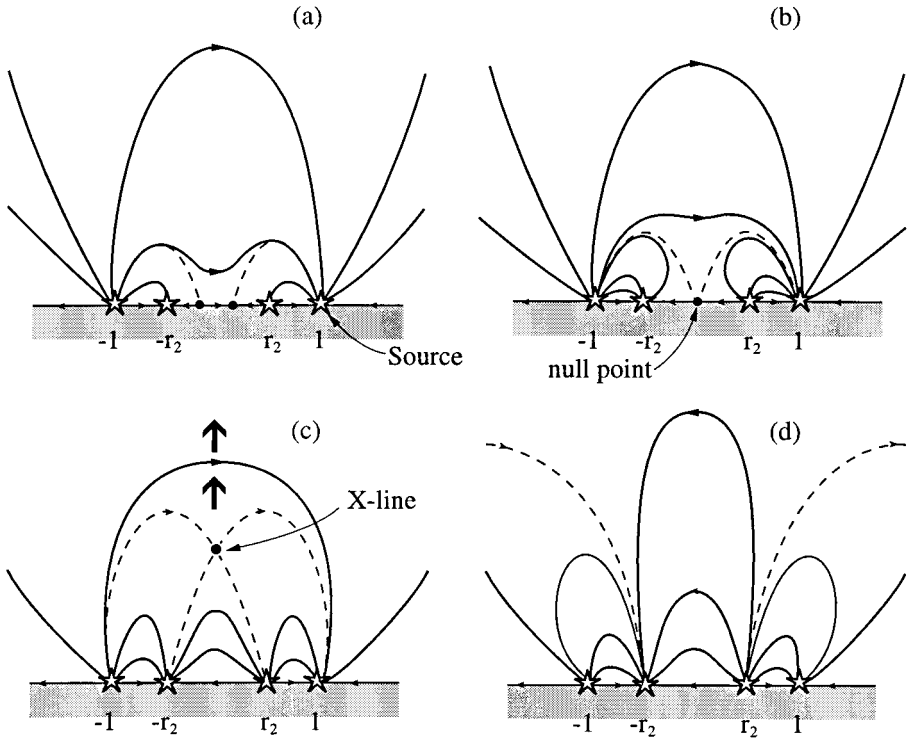

Figure 12. Emerging flux breakout in two dimensions due to an increase in magnetic flux at $-r_2$ and r_2.

be seen clearly. (Of course, if the field lines are potential, we cannot prescribe both footpoints of a field line as the sources move around, and so the choice of which field line directions at the source to keep fixed is entirely arbitrary.) Then we added a third (Figure 14(b)) and fourth (Figure 14(c)) source and as the sources move slowly around, a rapid counter-flipping of the field lines can be seen due to fan reconnection or separator reconnection. The flipping occurs as they reconnect and move close to the separatrix surface.

These simple experiments demonstrate a fundamental property of magnetic fields in association with magnetic reconnection: for reconnection that occurs on scales comparable to or larger than the characteristic separation of the magnetic poles (i.e., excluding the reconnection associated with small-scale footpoint motion resulting in what is generally described as field-line braiding), there are motions of pairs of field lines towards and later away from the reconnection site. In the simple simulations shown in Movie I on the CD-ROM, vacuum reconnection occurs through null points as field lines move through separators (the intersections of separatrix surfaces) whenever two pairs of field-line segments exchange connectivity at the reconnection location. The simulations suggest that most of the time field lines move through the coronal volume in response to source motions with

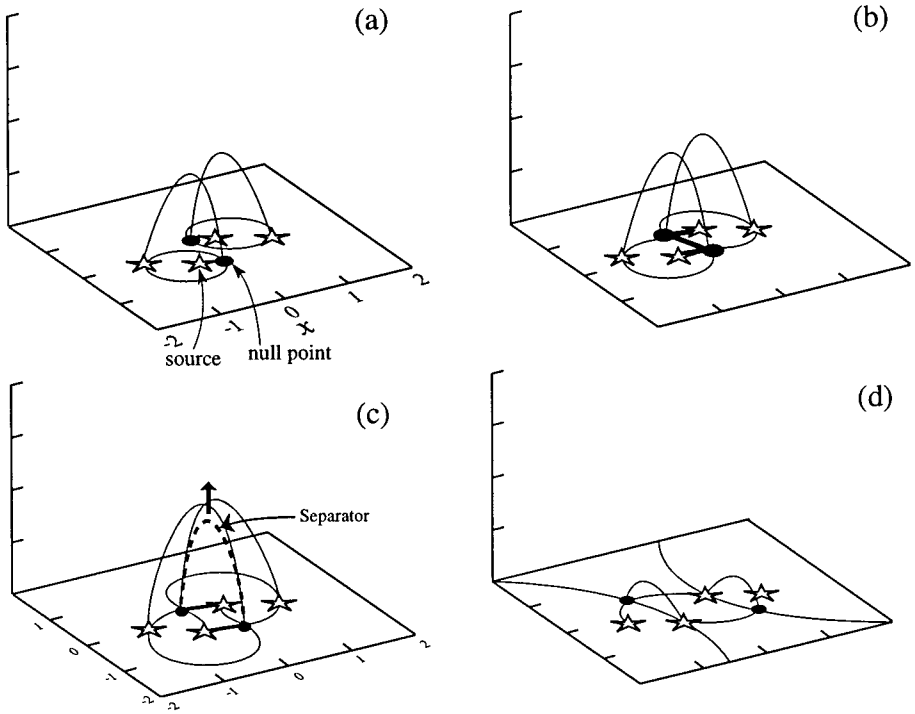

Figure 13. Emerging flux breakout in three dimensions.

speeds comparable in magnitude to that of the footpoints themselves. Just prior to reconnection, however, field lines approach the separator and slide past it often with a substantially increased speed. That speed decreases again after reconnection as the (new) field lines move away from the separatrix surface in their new domain of source connectivity. The potential-field simulations of the quiet-Sun corona (i.e., in a mixed-polarity region) suggest that the velocities just prior to and just after reconnection could easily be an order of magnitude larger than the source speeds (to be confirmed by detailed resistive-MHD simulations). In an active region, the velocities are generally much smaller because of the many surrounding sources of like polarity (as in the last segment of Movie I), but, in favorable conditions, substantial velocities can be expected there too.

6. Observations of Rapid Loop Motions

TRACE movies often show what appears to be the shifting of bright loops through the coronal volume. Schrijver *et al.* (1999) pointed out that the interpretation of this meandering is in many cases ambiguous: it may be caused by the geometrical evolution of the field or alternatively by the weaving of the heating through the

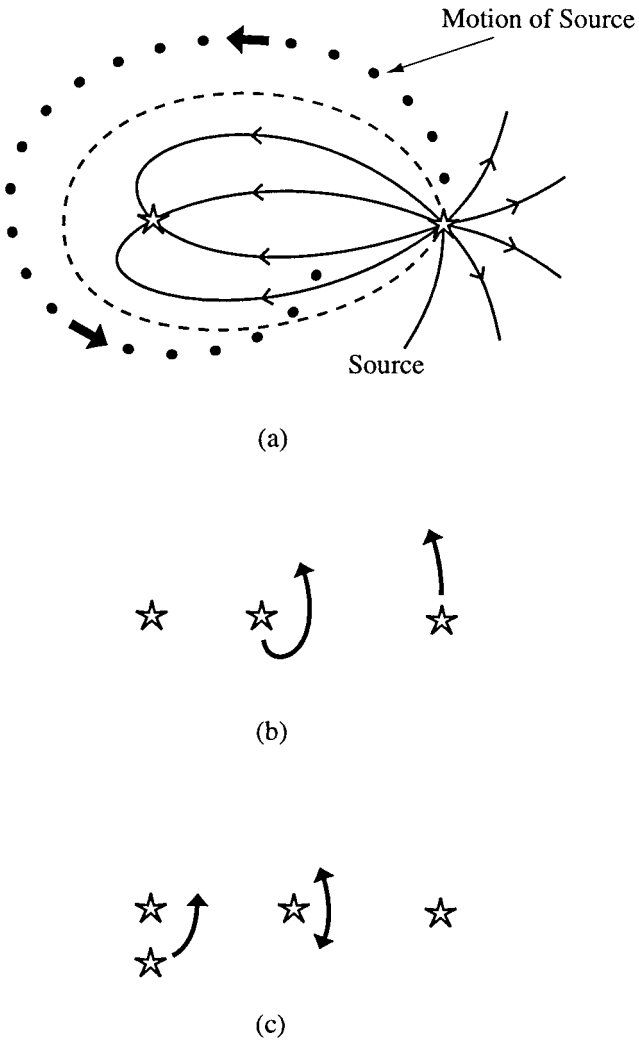

Figure 14. The configurations studied in the CD-ROM.

coronal volume, shifting around for periods of up to a few tens of minutes and lighting up subsequent field lines. In fact both appear to occur.

In this section we concentrate on a sample sequence showing what appears to be shifting loops. Movie II on the CD-ROM shows a 9-h sequence of observations taken with TRACE in the 171 Å passband (sample images are shown in Figure 15). If played at a sufficiently large speed, the movie gives the distinct impression that loops are shifting through the corona, even though most individual loops can be followed for only a limited duration.

The most prominent examples of the motion of loops are identified in Figure 15 as D1 to D4. The loops labeled D1 in Figure 15(a) and D2 in Figure 15(b) shift

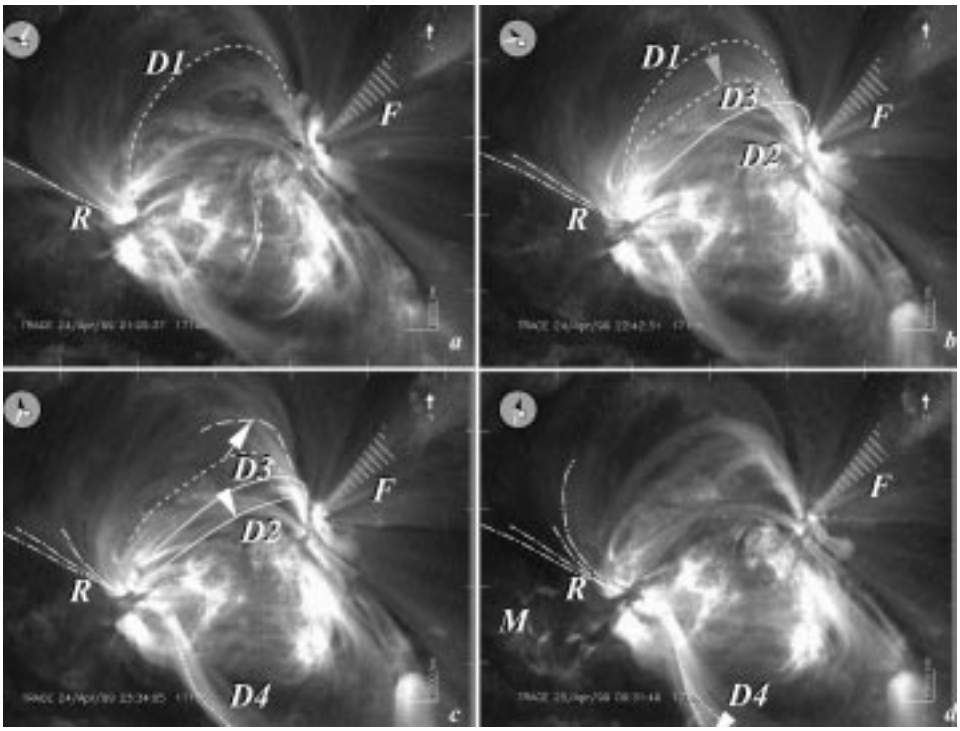

Figure 15. Four frames (numbers 95, 226, 276, and 354) taken from Movie II on the accompanying CD-ROM. The images are taken with TRACE in the 171 Å passband, on 24 April 1999. The times are given in the lower left-hand corner of each panel. The image covers 640 × 480 pixels; one pixel corresponds to 0.5 arc sec. The tick marks are spaced by 100 pixels. North is up. The location on the disk is represented by a rectangle on the analogue clock. The bars in the lower right-hand corner are 15 000 km in length. The labels mark the following details discussed in the text: D1, . . . 4, loop displacements; F, the lower segment of a fan of high-arching loops; M, moss following a flare; R, reconnecting loops.

with an average speed of somewhat over 3 km s^{-1}. In view of the potential-field simulations discussed in Section 5, we point out that, as the loop ensemble near D2 shifts southward, loops near D3 appear to shift northward at about the same speed (these are possibly the same loops that initially moved south starting at D1, but this identity is hard to establish). The loop movement is substantially larger than the typical speed at which loop footpoints are moved, particularly when averaged over 1.5 hr. This fact, and the apparent counter-moving loops at D2 and D3 appear to match the predictions of the potential-field simulations, and thus support the notion that some persistent (although possibly intermittent) reconnection of the large-scale field occurs even in the absence of obvious flaring. Such rapid loop motions can occur without a major reconfiguration of the large-scale field. In this respect it is of interest to note that the loop fan labeled F, anchored near the apparent footpoints of

loops near D1, D2, and D3, evolves in brightness throughout the movie, but does not change noticeably in shape.

That flare-like activity is also associated with large-scale reconnection is also evident from the movie. Around 00:20 UT on 25 April 1999 (frame 338 in Movie II) a patch of rapidly evolving 'moss' (emission from the top domain of the transition region, see Schrijver *et al.* (1999) for a description) develops in the lower-left corner of the images (near label M in Figure 15(d)). Such moss is often associated with flares (which are often missed or seen with difficulty with TRACE because of its soft bandpass). Large-scale reconnection appears to occur for the loops near label R: the distortion that occurred throughout the movie is seen to accelerate and the loops seem to swing around from an eastward to a westward direction.

7. Conclusions

We have presented the essence of a new exact solution for reconnective annihilation, whose detailed properties will be reported in future. Also, the process of reconnection at 3D null points by spine reconnection, fan reconnection and separator reconnection is described. In particular, separator reconnection may follow the natural collapse of the separator into a current sheet. Furthermore, the rate of reconnection of two approaching flux tubes is estimated. It is stressed that the enormous complexity of the coronal magnetic field may be unraveled by focusing on the skeleton of the field. In particular, reconnection events such as heating of bright points may be triggered by changes of topology (see Brown and Priest, 1999).

There are many observational signatures of reconnection, including:

– heating (as in for instance nanoflares, see Parnell and Aschwanden, these proceedings);

– fast jets of plasma (such as those seen by *Yohkoh* (Shibata *et al.*, 1996) and as explosive events by Sumer (Innes *et al.*, 1997));

– cusps and interacting loops (especially by the Soft X-ray Telescope on *Yohkoh* (Yoshida and Tsuneta, 1976));

– the creation of twist in a loop by the conversion of mutual magnetic helicity to self-helicity (see Chae, these proceedings); and, as we have seen, rapid motions of field lines, especially near separatrix surfaces (see the attached movie).

Now, what is likely to happen in quiet-Sun large-scale (i.e., non-braiding) reconnection in response to source motions? Energy that is released in such a reconnection process is deposited on the field line immediately following reconnection. That energy is likely to reach the chromosphere (either as particle beams or through conduction) within a few minutes for typical quiet-Sun field lines. Chromospheric material then rises into the loop by the increase in the pressure scale-height on a time-scale of a minute or so, upon which the loop becomes visible in the EUV passband. The energy that is deposited in the reconnection process is radiated away

on a time-scale that is substantially longer than the conductive time-scale. The visibility of the loop at any one temperature (i.e., in a narrow-band instrument such as TRACE) will be shorter than the cooling time-scale, depending on how fast the temperature decreases through the range for which the instrument is sensitive.

If the large-scale reconnection in response to substantial footpoint motions were to deposit a significant fraction of the coronal energy budget along the reconnecting field lines, these should consequently show up as they move through the coronal volume. If this heating were fairly continuous, then a set of successively heated field lines should light up outlining a shell-like surface in the vicinity of the separatrix surfaces. If the heating were intermittent, then rapidly moving loops would be seen, shifting over several thousands of kilometers in a quarter of an hour (the typical radiative cooling time-scale). Neither appear to be observed in quiet-Sun movies, but we still need to establish whether the cadence and sensitivity of TRACE suffice to see the expected displacements, or whether there are indeed expected to be only a few overlying separatrix shells in any line of sight so as not to drown the signal of any individual shell in the overall emission. But while awaiting these results, it seems that the observations to date do not support the notion that *large-scale* reconnection in response to substantial footpoint displacements is responsible for a substantial fraction of the coronal heating over quiet Sun. Instead, it may well be caused by small-scale reconnection in many current sheets spread throughout the volume.

Clearly, our exploration of the many new features of three-dimensional reconnection has only just begun (Priest and Forbes, 2000) and will continue to be a hot topic in future.

References

Bungey, T. N.: 1995, PhD Thesis, St Andrews University.

Brown, D. and Priest, E. R.: 1999, *Solar Phys.* **190**, 25 (this issue).

Craig, I. J. D. and Henton, S. M.: 1995, *Astrophys. J.* **450**, 280.

Handy, B. N., Acton, L. W., Kankelborg, C. C., Wolfson, C. J., Akin, D. J., Bruner, M. E., Carvalho, R., Catura, R. C., Chevalier, R., Duncan, D. W., Edwards, C. G., Feinstein, C N., Freeland, S. L., Friedlander, F. M., Hoffman, C. H., Hurlburt, N. E., Jurcevich, B. K., Katz, N. L., Kelly, G. A., Lemen, J. R., Levay, M., Lindgren, R. W., Mathur, D. P., Meyer, S. B., Morrison, S. J., Morrison, M. D., Nightingale, R. W., Pope, T. P., Rehse, R. A., Schrijver, C. J., Shine, R. A., Shing, L., Strong, K. T., Tarbell, T. D., Title, A. M., Torgerson, D. D., Golub, L., Bookbinder, J. A., Caldwell, D., Cheimets, P. N., Davis, W. N., Deluca, E. E., McMullen, R. A., Amato, D., Fisher, R., Maldonado, H., and Parkinson, C.: 1999, *Solar Phys.* **187**, 229.

Innes, D. E., Inhester, B., Axford, W. I., and Wilhelm, K.: 1997, *Nature* **386**, 811.

Parnell, C. E., Smith, J., Neukirch, T., and Priest, E. R.: 1996, *Phys. of Plasmas* **3**, 759.

Priest, E. R. and Forbes, T. G.: 2000, *Magnetic Reconnection: MHD Theory and Applications*. Cambridge University Press, Cambridge, UK.

Priest, E. R. and Titov, V. S.: 1996, *Phil. Trans. Roy. Soc.* **354**, 2951.

Priest, E. R., Titov, V. S., Grundy, R. E., and Hood, A. W.: 1999, *Proc. Roy. Soc.*, in press.

Schrijver, C. J., Shine, R. A., Hurlburt, N. E., Tarbell, T. D., and Lemen, J. R.: 1997, 'The Dynamic Quiet Solar Corona: 4 Days of Joint Observing with EIT and MDI', in O. Kjeldseth-Moe and A. Wilson (eds), *Proceedings of the 5th SOHO Workshop, Oslo, June 1997*, ESA SP-404, pp. 669–674.

Schrijver, C. J., Title, A. M., Berger, T. E., Fletcher, L., Hurlburt, N. E., Nightingale, R., Shine, R. A., Tarbell, T. D., Wolfson, J., Golub, L., Bookbinder, J. A., DeLuca, E. E., McMullen, R. A., Warren, H. P., Kankelborg, C. C., Handy, B. N. and De Pontieu, B.: 1999, *Solar Phys.* **187**, 261.

Shibata, K., Shimojo, M., Yokoyama, T., and Ohyama, M.: 1996, 'Theory and Observations of X-Ray Jets', in R. D. Bentley and J. T. Mariska (eds), *Magnetic Reconnection in the Solar Atmosphere*, pp. 29–38.

Sonnerup, B. U. O. and Priest, E. R.: 1975, *J. Plasma Phys.* **14**, 283.

Yoshida, T. and Tsuneta, S.: 1996, *Astrophys. J.* **459**, 342.